Yamamoto, K., & Sekine, T. (1979b) J. Biochem. (Tokyo) 86, 1869–1881.
Yamamoto, K., & Sekine, T. (1980) J. Biochem. (Tokyo) 87, 219–226.
Yamamoto, K., & Sekine, T. (1983) J. Biochem. (Tokyo) 94, 2075–2078.
Yamamoto, K., & Sekine, T. (1986) J. Biochem. (Tokyo) 99, 199–206.

ADP Release Is Rate Limiting in Steady-State Turnover by the Dynein Adenosinetriphosphatase†

Erika L. F. Holzbaur and Kenneth A. Johnson*
Department of Molecular and Cell Biology, 301 Althouse Laboratory, Pennsylvania State University, University Park, Pennsylvania 16802

Received July 12, 1988; Revised Manuscript Received November 10, 1988

ABSTRACT: The kinetics of the product release steps in the pathway of ATP hydrolysis by dynein were investigated by examining the rate and partition coefficient of phosphate–water ^{18}O exchange under equilibrium and steady-state conditions. Dynein catalyzed both medium and intermediate phosphate–water oxygen exchange with a partition coefficient of 0.30. The dependence of the rate of loss of the fully labeled phosphate species on the concentration of ADP was hyperbolic, with an apparent K_d for the binding of ADP to dynein of 0.085 mM. The apparent second-order rate constant for phosphate binding to the dynein–ADP complex was 8000 M^{-1} s^{-1}. The time course of medium phosphate–water oxygen exchange during net ATP hydrolysis was examined in the presence of an ATP regeneration system. The observed rate of loss of $P^{18}O_4$ was comparable to the rate observed at saturating ADP which implies that ADP release is rate limiting for dynein in the steady state. Product inhibition of the dynein ATPase was also examined. ADP inhibited the enzyme competitively with a K_i of 0.4 mM. Phosphate was a linear noncompetitive mixed-type inhibitor with a K_i of 11 mM. These data were fit to a model in which phosphate release is fast and is followed by rate-limiting release of ADP, allowing us to define each rate constant in the pathway. A discrepancy between the total free energy calculated compared to the known free energy of ATP hydrolysis suggests that there is an additional step in the pathway, perhaps involving a change in conformation of the enzyme–ADP state preceding ADP release.

Dynein couples the energy of ATP hydrolysis to drive the sliding of adjacent microtubules in the axoneme. This sliding is coordinated to produce the motive force for the beating of eukaryotic cilia and flagella. In previous work on the pathway for ATP hydrolysis by dynein (Scheme I), the rates of ATP binding, k_1, and hydrolysis, k_2, were determined by chemical quench flow studies to be 4.7×10^6 M^{-1} s^{-1} and 55 s^{-1}, respectively (Johnson, 1983), and indicated that product release was rate limiting in the reaction pathway. The kinetics of vanadate inhibition of the dynein ATPase suggested that phosphate release preceded ADP release (Shimizu & Johnson, 1983a), and it was implied, without proof, that phosphate release was rate limiting.

Scheme I

$$D + ATP \underset{k_{-1}}{\overset{k_1}{\rightleftharpoons}} D\text{–}ATP \underset{k_{-2}}{\overset{k_2}{\rightleftharpoons}} D\text{–}ADP\text{–}P_i \underset{k_{-3}}{\overset{k_3}{\rightleftharpoons}} D\text{–}ADP \underset{k_{-4}}{\overset{k_4}{\rightleftharpoons}} D + ADP$$

In the microtubule–dynein ATPase pathway, the binding of ATP induces the dissociation of the microtubule–dynein complex. ATP hydrolysis occurs on the free dynein. Microtubule activation of the dynein ATPase was first described by Omoto and Johnson (1986) and shown to be due to the effect of microtubules in increasing the rate of product release. In order to complete our thermodynamic description of the pathway, it is important to determine whether the rate-limiting step during steady-state turnover is phosphate release or ADP release. Moreover, it is likely that the slow step may also be the site of regulation of the ATPase cycle in the axoneme.

We have examined the product release steps of the dynein ATPase, using the techniques of phosphate–water ^{18}O exchange. Dynein has been shown to catalyze both medium and intermediate exchange reactions (Barclay & Yount, 1972; Kuleva et al., 1983; Holzbaur & Johnson, 1986). In this report, the rate and extent of medium exchange catalyzed by dynein were examined under both equilibrium and steady-state conditions. The data fit a model in which phosphate release is fast, and ADP release is the slow step. We further tested this hypothesis by examining the exchange reactions under conditions in which the dynein ATPase is both activated and inhibited.

Dynein from *Tetrahymena* cilia has three heads and three ATP binding sites per molecule (Johnson & Wall, 1983; Johnson, 1983; Shimizu & Johnson, 1983b). Because it is possible that there is more than one mechanism for ATP turnover, the process of intermediate exchange was examined in an attempt to distinguish multiple pathways for ATP hydrolysis in solution. The observed isotopic distribution of the product phosphate resulting from the hydrolysis of [γ-^{18}O]ATP was compared to theoretical models in order to evaluate the

† This work was supported by NIH Grant GM26726. K.A.J. was supported by an Established Investigatorship from the American Heart Association with funds contributed in part by the Pennsylvania Affiliate.
* Author to whom correspondence should be addressed.

0006-2960/89/0428-5577$01.50/0 © 1989 American Chemical Society

mechanism of the dynein ATPase, and the possible effects of the multiple heads.

Experimental Procedures

Preparation of Proteins and Nucleotides. Dynein was prepared according to the method of Porter and Johnson (1983a). *Tetrahymena* 22S dynein was purified on sucrose gradients and then dialyzed into 50 mM tris(hydroxymethyl)aminomethane (Tris)[1] and 4 mM $MgCl_2$ for 3 h. Dynein concentrations were determined by the absorbance at 280 nm using an extinction coefficient of 0.97 cm^2/mg (D. Clutter, D. Stimpson, V. Bloomfield, and K. A. Johnson, unpublished results). A molecular weight for dynein of 750000 per site has been determined by active-site titration experiments (Johnson, 1983; Shimizu & Johnson, 1983b) and was used to calculate the molar concentrations for the experiments described.

Myosin subfragment 1 (S-1) was produced by chymotryptic digestion of myosin isolated from rabbit back and leg muscles. The S-1 was purified by chromatography on DEAE-Sephacel (Weeds & Taylor, 1975). The concentration of the chymotryptic S-1 myosin was determined by the absorbance at 280 nm using an extinction coefficient of 0.75 cm^2/mg (Weeds & Pope, 1976).

ADP and ATP were purified by chromatography on DEAE-Sephadex with an elution gradient of 0.3–0.6 M triethylammonium bicarbonate. The purity of the nucleotides was verified by thin-layer chromatography on PEI–cellulose developed with 0.85 KH_2PO_4, and by HPLC analysis on a C_{18} column with a mobile phase of 0.1 M K_2HPO_4, 0.025 M tetrabutylammonium hydrogen sulfate, and 18% methanol at pH 7.2.

ATP Regeneration System. In some experiments, the ATP concentration was maintained by a regeneration system of 10 units/mL pyruvate kinase, 2 mM phosphoenolpyruvate, and 25 mM KCl in 50 mM Tris/4 mM $MgCl_2$ buffer at pH 7.5. The pyruvate kinase concentration was determined to be sufficient to maintain the level of ATP at the highest concentration of the dynein ATPase used.

ATPase Activity Assays. ATP hydrolysis rates were measured routinely by using the malachite green phosphate assay (Lanzetta et al., 1979) as described (Holzbar & Johnson, 1986). For some experiments, the time course of [γ-^{32}P]ATP hydrolysis was monitored. Charcoal columns were used to separate the resulting [^{32}P]phosphate, as described by Johnson (1983). Alternatively, 7 units/mL lactate dehydrogenase and 0.2 mM NADH were added to the ATP regeneration system, and the disappearance of NADH was monitored as the decrease in absorbance at 340 nm.

Preparation of [^{18}O]P_i and [γ-^{18}O]ATP. [^{18}O]P_i was prepared by reacting PCl_5 with 99% $H_2{}^{18}O$ obtained from Miles Laboratories (Risley & Van Etten, 1978), followed by ion-exchange chromatography on a Bio-Rad AG1-X8 (Cl^- form) column (Hackney et al., 1980). The resulting phosphate had an enrichment of 97% ^{18}O.

[γ-^{18}O]ATP was synthesized by the method of Mokrasch et al. (1960). [^{18}O]P_i was first reacted with KCNO followed by the addition of carbamate kinase and ADP. The resulting labeled ATP was purified as described, and the purity was checked by thin-layer chromatography. The enrichment of the resulting ATP was determined by Si-1 myosin hydrolysis of the Ca^{2+} salt of the labeled ATP. This reaction is known to occur with the incorporation of only a single water oxygen into the product phosphate (Levy & Koshland, 1959; Sleep et al., 1978).

Phosphate–Water Oxygen Exchange Methods. Exchange reactions were performed with 0.1 μM (0.075 mg/mL) dynein at 28 °C in 50 mM Tris/4 mM $MgCl_2$, pH 7.5. Tris buffer was used to avoid interference of anionic buffers (for example, HEPES or PIPES) during isolation of the phosphate. At each time point, an aliquot was removed from the reaction and vortexed with chloroform to denature the enzyme. Following extraction of the aqueous phases, ion-exchange chromatography was performed on Bio-Rad AG1-X8 (100–200 mesh, Cl^- form) to isolate the phosphates from each sample (Hackney et al., 1980). The samples were made basic by addition of Tris base and then were loaded onto 0.8 by 4 cm columns. After the columns were washed with 4 mL of 10 mM HCl, the samples were eluted with 10 mL of 30 mM HCl. The purified phosphates were concentrated by lyophilization and then were resuspended in approximately 20 μL of 95% ethanol.

Diazoethane was used to derivatize the phosphates for gas chromatograph–mass spectral analysis. The diazoethane was prepared prior to use from *N*-ethyl-*N'*-nitro-*N*-nitrosoguanidine from Aldrich Chemical Co. (Domanico et al., 1985). The precursor was dissolved in a cold solution of 40% KOH and diethyl ether and then distilled. Phosphate samples were reacted with the diazoethane for 30 min at room temperature. The ethylated phosphates were dried by addition of chloroform followed by concentration to approximately 20 μL under a stream of nitrogen gas. Crystals of sodium sulfate were added to further dry the samples prior to mass spectral analysis.

Gas Chromatography–Mass Spectrometry. The derivatized phosphates were analyzed by electron impact on a Finnigan 3200 quadrupole GC–MS with a Model 6000 data reduction system. The isotopes were separated on a 10% Silar 10C on a 100–120-mesh Gas Chrom Q column (Applied Science) at 150 °C. The isotopic cluster at *m/e* 99 was monitored by a modification of the method of Sharp and Benkovic (1979). The integrated peaks were used to calculate the relative concentrations of $P^{18}O_4$, $P^{18}O_3{}^{16}O$, $P^{18}O_2{}^{16}O_2$, $P^{18}O^{16}O_3$, and $P^{16}O_4$ with an error of ±1%.

Data Analysis. The observed [^{18}O]P_i distributions were compared to theoretical distributions calculated with a computer program based on transition probability functions modified from the work of Hackney (1980). Further modifications in the program allowed the calculation of theoretical distributions which best fit the data from the experiment of medium exchange during net ATP hydrolysis described below. The program iteratively approached a best fit to the observed distributions of the labeled phosphates while allowing the relative concentration of unlabeled phosphate to vary. This method allows the separation of the two pathways for accumulation of $P^{16}O_4$: from the exchange of water oxygens into the labeled phosphate and from the hydrolysis of unlabeled ATP. The distributions calculated by this program gave a good fit to the exchange data and to the measured rate of ATP hydrolysis by the dynein ATPase.

In order to avoid phosphate contamination, all exchange reactions were performed in acid-washed glassware. Deionized, distilled water was used. The triethylamine, diazoethane, ethanol, and chloroform were distilled in acid-washed glassware.

Results

Effect of ADP on Medium Phosphate–Water Oxygen Exchange. Dynein has been shown to catalyze medium exchange

[1] Abbreviations: NEM, *N*-ethylmaleimide; Tris, tris(hydroxymethyl)aminomethane.

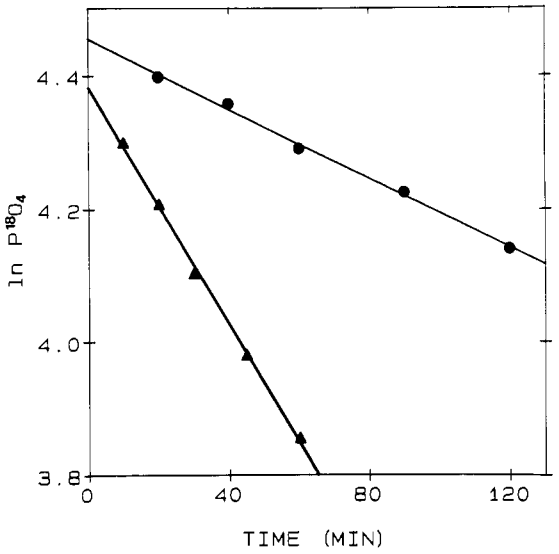

FIGURE 1: Effect of ADP concentration on the rate of loss of $P^{18}O_4$. Dynein at 0.1 μM was reacted with 0.028 mM ADP (●), or 2.85 mM ADP (▲), and 20 mM $P^{18}O_4$ in 50 mM Tris/4 mM $MgCl_2$, pH 7.5 at 28 °C.

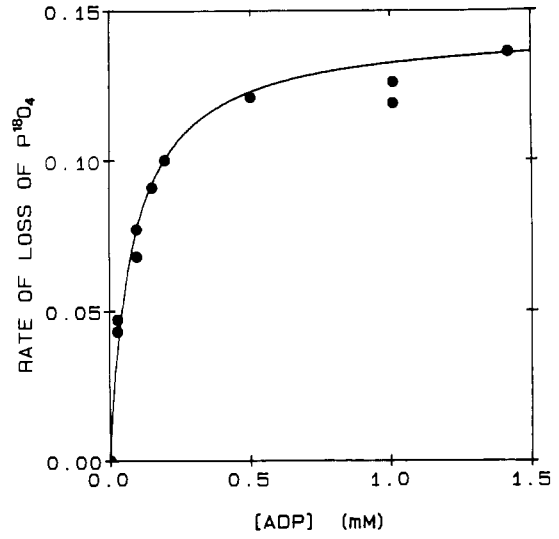

FIGURE 2: Rate of medium exchange as a function of ADP concentration. The rate of loss of $P^{18}O_4$ ($s^{-1} \times 10^3$) during medium exchange catalyzed by dynein was measured at varying ADP concentrations as described in Figure 1. The data can be fit to a hyperbola with a half-maximal rate at 0.085 mM and a maximum rate of 1.4×10^{-4} s^{-1}.

of phosphate oxygen in the presence of ADP (Kuleva et al., 1983; Holzbaur & Johnson, 1986). The dependence of the rate of this exchange upon the concentration of ADP was first determined. Medium exchange reactions were performed with 0.1 μM dynein and 20 mM $P^{18}O_4$ in 50 mM Tris/4 mM $MgCl_2$, pH 7.5 at 28 °C. Representative time courses of the disappearance of the fully labeled phosphate species at 0.028 and 2.85 mM ADP are shown in Figure 1. The rate of loss of $P^{18}O_4$ as a function of the ADP concentration is shown in Figure 2. The data can be fit to a hyperbola, with a half-maximal rate at 0.085 mM ADP and a maximum rate at saturating ADP of 1.4×10^{-4} s^{-1}.

Partition coefficients were calculated for each reaction according to the equation $P_c = (4 - R_4)/3$ where R_4 is the rate of loss of $P^{18}O_4$ divided by the rate of decrease in the average ^{18}O enrichment of the phosphate (Hackney et al., 1980). The partition coefficient was not found to vary significantly with the ADP concentration. The average value for all determinations was 0.27 ($s_{n-1} = 0.04$, $n = 13$).

Table I: Effect of [P_i] on the Rate of Medium Exchange[a]

[P_i] (mM)	rate (s^{-1})	additions
1	2.0×10^{-4}	
1	2.0×10^{-4}	1 μM Ap_5A
1	1.4×10^{-4}	50 mM KCl
5	1.4×10^{-4}	
10	1.4×10^{-4}	
20	1.4×10^{-4}	

[a] The reactions were performed with 0.1 μM dynein, 2 mM ADP, and varying concentrations of phosphate in the absence and presence of 1 μM Ap_5A and 50 mM KCl in 50 mM Tris4 mM $MgCl_2$, pH 7.5 at 28 °C.

The rate of binding of phosphate to the D–ADP complex can be calculated from the rate of loss of the fully labeled phosphate species at saturating ADP. The first-order disappearance of $P^{18}O_4$ is described by $k_{-2}k_{+3}/(k_{-2} + k_{+3})$ (Sharp & Benkovic, 1979) or $P_c k_{-3}$ (Scheme I). Dividing the observed rate by the partition coefficient and by the dynein concentration yields a rate for phosphate binding of 8000 M^{-1} s^{-1}. This is in agreement with the estimate of this rate reported previously (Holzbaur & Johnson, 1986).

Effect of P_i on Medium Phosphate–Water Oxygen Exchange. It has been previously determined that the rate and extent of medium exchange by dynein are the same at 10 and 20 mM phosphate by using ^{31}P NMR to measure the resulting isotopic distributions of phosphate (Holzbaur & Johnson, 1986). Due to the greater sensitivity of the GC–mass spectrophotometry, it was possible to vary the phosphate concentration in these experiments from 20 mM down to 1 mM. The exchange reactions were performed with 0.1 μM dynein and 2 mM ADP. The observed rates of loss of $P^{18}O_4$ at various phosphate concentrations are summarized in Table I, showing no significant phosphate concentration dependence and therefore no saturation in the binding of phosphate.

An exchange reaction was run with the addition of 1 μM diadenosine pentaphosphate (Ap_5A), a highly specific inhibitor of adenylate kinase (Lienhard & Secemski, 1973; Feldhaus et al., 1975). Dynein which has not been sucrose gradient purified has been shown to contain a low but measurable level of this contaminating enzyme (Shimizu & Johnson, 1983a), although purified 22S dynein has not been shown to be contaminated (Holzbaur & Johnson, 1986). Even at the relatively high ADP concentration used in this experiment, there is no difference in the exchange patterns observed in the presence and absence of the adenylate kinase inhibitor.

A small decrease in the rate of loss of the fully labeled phosphate species was seen at phosphate concentrations of 5 mM and greater. It is possible that this observed decrease in the rate of exchange at the higher phosphate concentrations is due to the increased ionic strength of the reaction. The dynein ATPase has been shown to be activated at high ionic strength, although the evidence suggests that this activation is anion dependent and is maximal for Cl^- (Gibbons et al., 1985). Therefore, an exchange reaction was run at 1 mM $P^{18}O_4$ with 50 mM KCl; the rate of loss of the fully labeled phosphate species was the same as the exchange rates observed at 5, 10, and 20 mM phosphate (Table I).

Medium Exchange during Net ATP Hydrolysis. It was important to determine whether dynein can catalyze the time-dependent washout of labeled oxygen from phosphate to water during steady-state turnover of ATP. Such exchange would be due to the binding of phosphate to the enzyme–ADP intermediate and would be a function of the lifetime of that intermediate. A reaction was run with 0.1 μM dynein, 1 mM

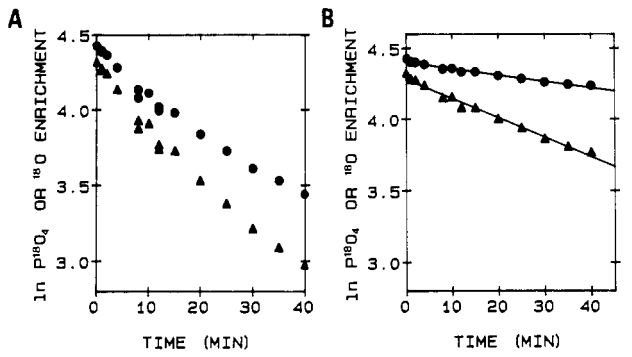

FIGURE 3: Medium exchange during net ATP hydrolysis. Dynein at 0.1 μM was reacted with 1 mM ATP and 1 mM $P^{18}O_4$ in the presence of a pyruvate kinase–phosphoenolpyruvate ATP regeneration system, in 50 mM Tris, 4 mM $MgCl_2$, and 25 mM KCl, pH 7.5 at 28 °C. (A) Time courses of loss of $P^{18}O_4$ (▲) and of the average ^{18}O enrichment (●). (B) Corrected rates of loss of $P^{18}O_4$ (▲) and average ^{18}O enrichment (●). The observed distributions were corrected for the dilution of the phosphate pool with unlabeled phosphate from the hydrolysis of ATP using an iterative fitting program as described under Results. The resulting curves are linear, and the slopes describe a partition coefficient of 0.34.

ATP, and 1 mM $P^{18}O_4$ in the presence of the ATP regeneration system. Under these conditions, the concentration of free ADP will be very low, and therefore any exchange due to the rebinding of ADP to the free enzyme should be insignificant (see Figure 2). Figure 3A shows the time course of the loss of the fully labeled phosphate species, and of the decrease in the average ^{18}O enrichment of the phosphate. The time courses show that dynein is catalyzing a relatively rapid exchange reaction. The apparent rate of this exchange is much too fast to be explained by medium exchange occurring due to the rebinding of ADP. However, to ensure that the concentration of free ADP was insignificant over the course of the exchange reaction, the pyruvate kinase concentration was doubled from 10 to 20 units/mL. No decrease in the rate of exchange was observed, which indicated that the medium exchange reaction observed during the steady-state hydrolysis of the ATP was not due to the rebinding of free ADP to the dynein. These data imply that the enzyme–ADP intermediate predominates during steady-state turnover, but this conclusion depends upon a more precise comparison of the rates of exchange during ATP turnover and the rate observed when the enzyme is saturated with ADP.

Quantitation of the exchange rate during ATP turnover is complicated because hydrolysis of the unlabeled ATP contributes to the generation of $P^{16}O_4$ and dilutes the phosphate pool over time. In order to differentiate the increase in the relative concentration of $P^{16}O_4$ due to exchange from the time-dependent accumulation of unlabeled phosphate due to the hydrolysis of unlabeled ATP, the isotopic distributions at each time point were subject to computer analysis. The program allowed the relative contribution of the unlabeled phosphate species to vary while iteratively solving for a best fit to a single partition coefficient for the labeled phosphate species. The resulting distributions have been replotted in Figure 3B as the time course of loss of $P^{18}O_4$ and of the average ^{18}O enrichment. The fitted data described a medium exchange reaction with a rate of loss of the fully labeled phosphate species of 2.3×10^{-4} s^{-1}, with a fit to a single partition coefficient of 0.34. The rate is comparable to that seen with dynein fully saturated with ADP, thus implying that a large fraction of the dynein sites are occupied by ADP during ATP turnover and thereby demonstrating that ADP release must be rate limiting.

Because KCl has been shown to increase the rate of the dynein ATPase, the experiment was repeated using potassium acetate (K^+ is a required activator of pyruvate kinase). The reaction of medium exchange during net ATP hydrolysis was run starting with saturating or subsaturating unlabeled ATP. The initial concentration of $P^{18}O_4$ was increased to 5 mM in order to more accurately determine the rate of exchange against an accumulating background of unlabeled phosphate. To verify the accuracy of the assumptions involved in the calculations, the increase in total phosphate concentration over time was monitored by withdrawing aliquots from the exchange reaction at various time points. After the enzyme was quenched with 1 N perchloric acid, the phosphate concentrations of the time points were determined by the malachite green assay (Lanzetta et al., 1979). The isotopic distribution of the phosphate at each time point was determined by mass spectral analysis. Then the data were corrected directly for the dilution of the labeled phosphate pool due to ATP hydrolysis. The resulting time course for exchange at 0.1 μM dynein, 1 mM ATP, and 5 mM $P^{18}O_4$ gave a rate of loss of the fully labeled phosphate species of 1.3×10^{-4} s^{-1}. The best-fit partition coefficient was determined to be 0.29.

The rates of exchange during net ATP hydrolysis can be compared to the results observed for medium exchange at saturating ADP and 1 mM phosphate. The similarities in both rates of exchange in the two experiments imply that the same exchange reaction is occurring under both sets of conditions. Both experiments resulted in phosphate distributions which could be fit to a single partition coefficient of 0.3. The rate of exchange observed in the presence of ATP was 90% of that observed at 2.85 mM ADP (Figure 1). Thus, it can be argued that during ATP hydrolysis, the D–ADP complex is the predominant form in solution. Kinetically, this would result if ADP release is the rate-limiting step in the dynein ATPase pathway.

Effect of Glycerol on Medium Exchange during Net ATP Hydrolysis. Glycerol has been shown to inhibit the dynein ATPase (Shimizu & Katsura, 1988), with about 50% inhibition of the steady-state turnover rate observed at a concentration of 15% (v/v) glycerol. It was also shown that glycerol affects the extent of medium phosphate–water oxygen exchange, with the partition coefficient increasing at increased glycerol concentrations. Therefore, we decided to investigate the effects of glycerol on the reaction of medium exchange during net ATP hydrolysis.

The exchange reaction was run in the presence of 15% glycerol to yield 58% inhibition of steady-state ATP hydrolysis under these conditions. Dynein, at a concentration of 0.1 μM, was reacted with 1 mM ATP and 5 mM $P^{18}O_4$ in the presence of 15% (v/v) glycerol and with 40 units/mL pyruvate kinase, 2 mM phosphoenolpyruvate, and 25 mM potassium acetate in 50 mM Tris/4 mM $MgCl_2$ buffer at pH 7.5 and 28 °C. It was necessary to increase the pyruvate kinase concentration from 10 to 40 units/mL, as the activity of this enzyme was also inhibited by glycerol. The increase in phosphate concentration with time was measured in order to correct the observed isotopic distributions for the dilution of the phosphate pool due to the hydrolysis of unlabeled ATP. In the presence of 15% glycerol, the rate of loss of the fully labeled phosphate species was 8.8×10^{-4} s^{-1}, and the ratio of the rate of loss of $P^{18}O_4$ to the rate of loss of the average ^{18}O enrichment described a partition coefficient of 0.48.

A comparison of the isotopic distribution of the phosphate to a theoretical distribution calculated from a best-fit partition coefficient of 0.48 is shown in Figure 4. The partition

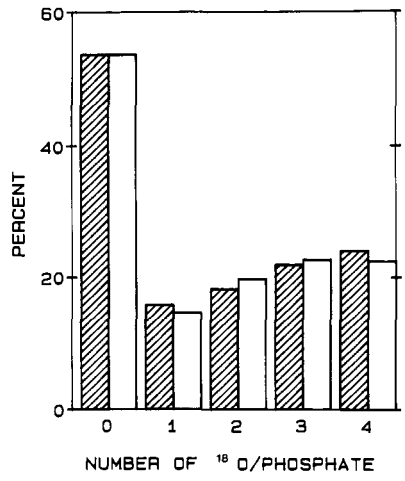

FIGURE 4: Medium exchange during net ATP hydrolysis in the presence of glycerol. A comparison of the corrected isotopic distribution of the phosphate (hatched bars) to the theoretical distribution calculated from a best-fit partition coefficient of 0.48 (white bars).

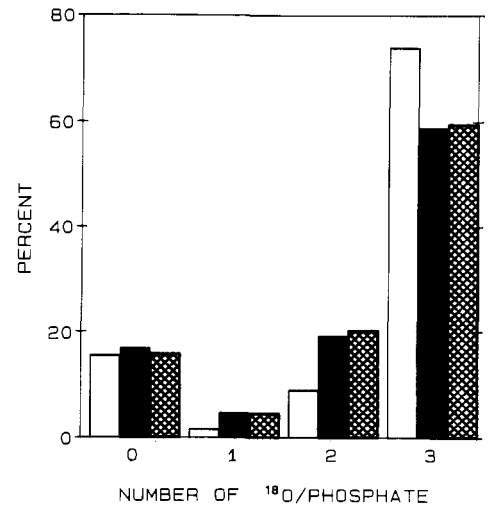

FIGURE 5: Intermediate exchange by dynein. The exchange reaction was run with 0.1 μM dynein and 1 mM [γ-^{18}O]ATP in 50 mM Tris/4 mM $MgCl_2$, pH 7.5 at 28 °C. The isotopic distribution at 0.75 min (black bars) is shown with the best-fit theoretical distribution (cross-hatched bars) of 0.25. Also shown is the initial distribution of the labeled ATP, as determined by the Ca^{2+}-activated ATPase of myosin subfragment 1 (white bars).

coefficient is altered, and so k_3 may be inhibited in the presence of glycerol. However, because exchange was observed during the course of net ATP hydrolysis, the D–ADP complex must still have a significantly long lifetime in solution.

Medium Exchange by NEM-Modified Dynein. The ATPase activity of dynein isolated from *Tetrahymena* has been shown to be increased by treatment with *N*-ethylmaleimide (NEM) (Blum & Hayes, 1974; Shimizu & Kimura, 1974, 1977; Shimizu, 1979b). However, the mechanistic basis for the approximately 3-fold activation observed is unknown. Thus, the phosphate–water oxygen exchange reactions of NEM-treated 22S dynein were investigated.

For the medium exchange reaction, 22S dynein was incubated with and without 0.5 mM NEM for 16 h on ice. Both the unmodified and the NEM-treated dynein were then made 1 mM in dithiothreitol to stop the reaction. The treatment with NEM resulted in a 2.7-fold activation of the ATPase activity over the control rate. Both the modified and the unmodified dynein samples were incubated at 0.1 μM with varying concentrations of ADP and 20 mM $P^{18}O_4$ in 50 mM Tris/4 mM $MgCl_2$ buffer at pH 7.5 and 28 °C. The observed rate of exchange was inhibited by the treatment of the enzyme with the alkylating agent. At 1 mM ADP, the rate of loss of $P^{18}O_4$ catalyzed by the unmodified enzyme was 1.6×10^{-4} s^{-1}. The rate for the NEM-treated dynein was 9×10^{-6} s^{-1}, representing an 18-fold inhibition by NEM treatment. At 4 mM ADP, the corresponding rates were 1.9×10^{-4} and 2×10^{-5} s^{-1} for the unmodified and modified dynein, respectively, which represent a 9-fold inhibition by pretreatment with NEM. The results from both enzyme preparations could be described by a partition coefficient of 0.3. However, the observed extent of exchange by the modified enzyme was too small to accurately determine this value. An analysis of the change in the isotopic distributions with time showed that the partition coefficient did not appear to be altered by the treatment with NEM. The partition coefficient for the exchange reaction is defined as $k_{-2}/(k_{-2} + k_3)$. If k_{-2} is assumed to be unaffected by the alkylation reaction, and if k_3 was activated by treatment of the dynein with NEM, then a lower partition coefficient would have been observed. Because the partition coefficient was not lower for the modified dynein and the ratio of k_{-2}, it appears that the binding of ADP may have been weakened. This implies that the faster ATP turnover observed for the modified dynein may be due to an increase in k_4, the rate of release of ADP from the enzyme.

The reaction of medium exchange during net ATP hydrolysis was also run with dynein which had been incubated overnight with 0.5 mM NEM, as described above. The observed specific activity of the dynein was activated 3.5-fold as measured in the pyruvate kinase–lactate dehydrogenase spectrophotometric coupled assay. The exchange reaction was run with 0.1 μM dynein, 1 mM ATP, and 5 mM $P^{18}O_4$ in the presence of 10 units/mL pyruvate kinase, 5 mM phosphoenolpyruvate, and 25 mM potassium acetate in Tris buffer at pH 7.5 and 28 °C. No medium phosphate–water oxygen exchange was observable in the time course of reaction with the NEM-treated enzyme.

Intermediate Exchange. Since the dynein ATPase catalyzes medium exchange during net ATP hydrolysis even in the presence of the pyruvate kinase–phosphoenolpyruvate ADP trapping system, it was difficult to obtain an intermediate exchange pattern which did not show the contributions of the medium exchange reaction. To minimize the extent of medium exchange, the intermediate exchange experiment was run for a short time to obtain a small fraction of conversion of ATP to products, and the product phosphate was pooled from a large volume.

The incorporation of water oxygens into the phosphate generated during the hydrolysis of [γ-^{18}O]ATP by dynein was examined. The exchange reaction was run with 0.1 μM dynein and 1 mM [γ-^{18}O]ATP in 50 mM Tris/4 mM $MgCl_2$, pH 7.5 at 28 °C. The reaction was stopped after 0.75 and 1.4 min by vigorously mixing with chloroform. The isotopic distributions of the product phosphate are shown in Figure 5. Also shown are the results of an exchange reaction run with the Ca^{2+}-activated ATPase of the chymotryptic subfragment 1 of myosin. This enzyme has been shown to catalyze the hydrolysis of ATP with the incorporation of only a single water oxygen into the product phosphate (Levy & Koshland, 1959; Sleep et al., 1978). The concentration of myosin S-1 in the exchange reaction was chosen in order to yield the same extent of hydrolysis as 0.1 μM dynein. This allowed a more accurate determination of the level of signal over a possible background of contaminating inorganic phosphates.

The phosphate distribution can be solved for a best-fit partition coefficient by using a program modified from the

work of D. Hackney (Hackney et al., 1980). The best fit to the data is also shown in Figure 5. A comparison of the fit to the data indicates that the observed distribution is skewed toward the less enriched isotopes. This additional incorporation of unlabeled water oxygens into the product phosphate is time dependent; increasing incorporation was observed at increasing times of reaction. The additional exchange is due to the washout of labeled oxygens from the product phosphate through the reaction of medium exchange with the enzyme–ADP complex, as was observed during the experiment of medium exchange during net ATP hydrolysis. The additional washout of labeled oxygens is not minimized by the addition of an ADP trapping system. An intermediate exchange reaction was run in the presence of ADP and pyruvate kinase starting with ^{18}O-labeled phosphoenolpyruvate (a generous gift of D. Hackney). This experiment also resulted in a skewed phosphate distribution (data not shown). Thus, it is likely that the time-dependent increase in water oxygen incorporation observed in the intermediate exchange reaction is due to the rebinding of phosphate to the D–ADP intermediate before ADP is released.

Analysis of the results from the intermediate exchange reactions of enzymes can lead to the identification of more than one pathway for ATP hydrolysis in solution. *Tetrahymena* 22S dynein has three heads, and all three heads are thought to bind ATP (Johnson & Wall, 1983; Shimizu & Johnson, 1983b; Chilcote & Johnson, 1986; Clutter & Johnson, 1986). However, the intermediate exchange data can be fit to a model with a single partition coefficient. This implies either that there is a single predominant reaction mechanism or that the multiple heads have similar rates of phosphate release and of ATP synthesis at the active site. Unfortunately, due to the difficulties described in fitting the data to a theoretical model, it is not possible to distinguish partition coefficients which were not very different.

Product Inhibition of the Dynein ATPase. The dependence of the rate of medium exchange on the concentration of ADP and phosphate can be compared to the product inhibition of the dynein ATPase. Inhibition of the rate of ATP hydrolysis by ADP and phosphate has been reported (Otokawa, 1973; Shimizu & Kimura, 1977; Holzbaur & Johnson, 1986), although higher concentrations of phosphate have been shown to activate the dynein ATPase (Shimizu & Kimura, 1977). To further investigate the mechanism of ATP hydrolysis by dynein, we sought to determine the modes of inhibition and the inhibition constants for ADP and phosphate.

Inhibition of the steady-state ATPase by ADP was measured as a function of the ATP concentration using [γ-^{32}P]-ATP. ADP inhibited the enzyme competitively, with a K_i of 0.4 mM. A replot of the slope of the reciprocal plot versus the ADP concentration was linear, indicating that the inhibition is purely competitive.

The inhibition of the dynein ATPase by phosphate was measured by using a spectrophotometric coupled assay of pyruvate kinase and lactate dehydrogenase. Replots of the observed inhibition (Figure 6) indicate that phosphate is a linear noncompetitive mixed-type inhibitor, with a K_i of 11 mM.

Discussion

Dynein has been shown to catalyze the exchange of oxygen atoms between phosphate and water in the presence of ADP (Barclay & Yount, 1972; Kuleva et al., 1983; Holzbaur & Johnson, 1986). This equilibrium exchange reaction occurs by reversal of the steady-state ATP hydrolysis pathway (Holzbaur & Johnson, 1986).

Quantitative analysis of the exchange was based upon a model where ATP hydrolysis proceeds via direct displacement with no phosphorylated enzyme intermediate. Analysis of the stereochemistry of the reaction by Shimizu and Johnson (1989) using ^{18}O-labeled thiophosphate analogues of ATP indicates that hydrolysis proceeds with inversion of configuration and thus supports this simple model. The theoretical models also presume that there is unhindered rotation of the enzyme-bound phosphate. Departures from this case would be apparent if the phosphate distribution data could not be adequately fit to a binomial distribution. As was shown previously, the fit is sufficiently good to indicate unhindered rotation of the phosphate.

The medium exchange reaction catalyzed by dynein showed a saturable dependence on the concentration of ADP and no direct dependence on the concentration of phosphate. The ADP concentration dependence of the rate of exchange can be fit to a hyperbola with an apparent K_d for ADP binding equal to 85 μM. The rate of phosphate binding to the D–ADP complex (k_{-3} in Scheme I) was calculated from the rate of loss of the fully labeled phosphate species at saturating ADP to give a value of 8000 M^{-1} s^{-1}, in agreement with the estimate reported previously (Holzbaur & Johnson, 1986). As shown in Table I, phosphate was not saturating under the conditions of the experiment, so this is a measure of the rate constant for phosphate binding.

Medium exchange was found to occur at a relatively rapid rate during the net hydrolysis of ATP under conditions in which the concentration of free ADP was negligible. These data suggest that the release of ADP is the rate-limiting step for the dynein ATPase. Phosphate is released first, and the D–ADP intermediate has a sufficiently long lifetime in solution that labeled phosphate can rebind and undergo exchange. The observed rate of loss of the fully labeled phosphate species in the experiment of medium exchange during net ATP hydrolysis is sufficiently fast that the D–ADP intermediate must be the predominant form of the enzyme during steady-state ATP hydrolysis.

The potent inhibition of the dynein ATPase by vanadate can also be explained by this model. Vanadate is known to inhibit the dynein ATPase after a single catalytic turnover (Shimizu & Johnson, 1983a). Following hydrolysis of bound ATP, phosphate is released, and vanadate then binds rapidly to the D–ADP intermediate before the dissociation of the ADP. The relatively slow breakdown of the D–ADP complex may explain in part why vanadate inhibits dynein 10^6-fold more rapidly than myosin.

This model for the kinetics of the dynein ATPase has many implications. Microtubules have recently been shown to activate the dynein ATPase, presumably by increasing the rate of the limiting step (Omoto & Johnson, 1986). If the limiting step is the release of ADP, then microtubules may activate this rate, and thus the M–D–ADP complex will have a shorter lifetime in solution than the D–ADP complex. Current data on the effects of microtubules on the exchange reactions support this postulate (E. L. F. Holzbaur and K. A. Johnson, submitted for publication).

The hypothesis that ADP release is rate limiting was further tested by investigating the exchange reactions under conditions in which the enzyme was inhibited or activated. Shimizu and Katsura (1988) have shown that the steady-state hydrolysis of ATP by dynein is inhibited by glycerol and that the partition coefficient for medium exchange increases with increasing glycerol concentrations. On the basis of these data, they proposed that phosphate release may be the limiting step

during turnover and that glycerol inhibits the dynein ATPase by slowing the rate of phosphate release. We examined the effect of glycerol on the reaction of medium exchange during net ATP hydrolysis. Under the conditions of the experiment, only the D–ADP complex generated during steady-state hydrolysis of ATP is available to catalyze exchange of the labeled phosphate. The results showed a significant rate of exchange with a partition coefficient of 0.48. The relatively high rate of exchange observed necessitates an alternate interpretation of the results of Shimizu and Katsura. Glycerol inhibits the dynein ATPase by inhibiting ADP release and thus lowering the rate of steady-state turnover.

We also examined the exchange reactions under conditions in which the dynein ATPase is activated. Dynein shows increased ATPase activity after various treatments such as aging, mild heating, and reaction with amino and sulfhydryl reagents (Blum & Hayes, 1974; Shimizu & Kimura, 1974; Shimizu et al., 1977; Shimizu, 1979a). In particular, the modification of 22S dynein by NEM has been well characterized (Shimizu & Kimura, 1977; Shimizu, 1979b). In the presence of ATP and in the absence of Mg^{2+} ions, the NEM-induced activation of the ATPase was blocked, which suggests that the modified sulfhydryl groups may be involved in nucleotide binding (Shimizu & Kimura, 1977). The rate of exchange catalyzed by the NEM-modified dynein was significantly slower than the rate observed for unmodified dynein, although the partition coefficient was not found to vary significantly between the two enzyme preparations. Also, in the reaction of medium exchange during net ATP hydrolysis, the dynein which had been reacted with NEM showed an activated rate of ATP hydrolysis but catalyzed no apparent exchange over the reaction time course. These data argue that NEM modification of dynein increases k_4, the rate of ADP release, supporting our conclusion that ADP release is rate limiting.

The intermediate exchange reaction catalyzed by dynein resulted in a phosphate distribution which can be fit to a theoretical model calculated from a single partition coefficient of 0.3. However, the dynein molecule is composed of three globular heads connected by strands to a common base. Titration of the pre-steady-state phosphate burst has indicated a molecular weight per site of 750000, or approximately three ATPase sites per 2 MDa. Preliminary results from azido-ATP labeling studies of *Tetrahymena* dynein have indicated that there are three different ATP binding sites, one on each heavy chain (Chilcote & Johnson, 1986). It has also been shown that at least two of the ATPase sites are composed of antigenically distinct polypeptides (Clutter & Johnson, 1986). However, ATP binding and hydrolysis transients can be fit to a model of a single ATPase. Therefore, it is particularly interesting to note that the intermediate exchange distribution can be fit to a single partition coefficient. The reaction of medium exchange during net ATP hydrolysis was run both at low and at high concentrations of ATP, about 0.7 and 200 times the K_m, respectively. Since the results from both these experiments showed a fit to a single partition coefficient, there is no evidence for differential partitioning along multiple reaction pathways. Therefore, if there are multiple ATPases, they must catalyze ATP hydrolysis with similar kinetic constants. Taken together, these data imply that the three different heads catalyze ATP turnover with similar rates for ATP binding, ATP hydrolysis, and synthesis at the active site, and phosphate release.

These results can be contrasted to the observations made on the exchange reactions of myosin. Heterogeneity observed in the exchange reactions of myosin and its proteolytic fragments was found to be due both to the presence of a contaminating ATPase in the preparation (Sleep et al., 1980) and to multiple pathways for ATP hydrolysis in solution (Hackney & Clark, 1985). The data for dynein show no such evidence for heterogeneity of catalysis due to either contamination or multiple kinetic pathways, but this has not been tested to the same degree of precision as for myosin.

Table II: Kinetic Constants of the Dynein ATPase Pathway[a]

reaction	forward	reverse	K_{eq}	$\Delta G°$ (kcal/mol)
ATP binding	4 μM^{-1} s^{-1}	0.15 s^{-1}	26.7 μM^{-1}	−6.2
ATP hydrolysis	100 s^{-1}	30 s^{-1}	3.3	−0.7
$E–ADP_1 \rightarrow E–ADP_2$				−4.2
ADP release	4 s^{-1}	0.015 μM^{-1} s^{-1}	267 μM	−1.3
P_i release	70 s^{-1}	8000 M^{-1} s^{-1}	8.75 mM	−2.0

steady-state kinetic parameter	value
K_m (Michaelis constant) (μM)	5
$K_{i,ADP}$ (M)	4×10^{-4}
$K_{i,P}$ (M)	1×10^{-2}
k_{cat} (turnover rate) (s^{-1})	4
V_{max} (sp act.) [μmol/(mg·min)]	0.4

[a] Kinetic constants consistent with all kinetic and exchange reactions measured are listed. The free energy change was calculated under the presumed physiological conditions: pH 7.0, 10^{-3} M ATP, 10^{-5} M ADP, and 10^{-3} M phosphate at 28 °C.

The patterns of exchange observed would be expected if product release is ordered with phosphate release followed by slower ADP release. This interpretation is supported by the product inhibition data. According to the pathway we have established for ATP hydrolysis by dynein, the K_i for ADP is equal to the K_d. The value of 0.4 mM is somewhat larger than the value of 0.1 mM determined from the dependence of the rate of medium exchange on the ADP concentration. As described below, the differences may be due to oversimplifications in the kinetic model. The K_i for phosphate is equal to the sum of the rates of phosphate and ADP release divided by the rate of phosphate binding, or $K_{i,P_i} = (k_3 + k_4)/k_{-3}$. If ADP release is assumed to be the limiting step during steady-state turnover, then from the K_i and the measured rate of phosphate binding a rate of phosphate release of about 80 s^{-1} can be calculated.

An estimate of the K_d for phosphate binding of 1×10^{-2} M can also be determined. However, if this value represents a true estimate of the K_d for phosphate, then it is unclear why saturation was not observed in the rate of washout of the label during medium exchange at 20 mM P_i. This discrepancy may be due to ionic strength effects under the conditions of the experiment. Alternatively, the discrepancy may indicate the presence of a second type of phosphate binding site on the dynein. Since the K_d for phosphate was not measured directly, there are no data to disprove this hypothesis. However, the most likely explanation may be that our current model for the ATP hydrolysis pathway is an oversimplification. A more complex scheme may be necessary to describe all the data. Such a model would include an additional D–ADP′ complex, which must isomerize prior to ADP release. As discussed below, the discrepancy in the thermodynamics of the pathway also supports this hypothesis.

The kinetic parameters of the dynein ATPase are summarized in Table II. These values were used to predict the turnover rates of the forward and reverse reactions according to the complete kinetic solution to the four-state model. The results were consistent with the experimentally observed rates

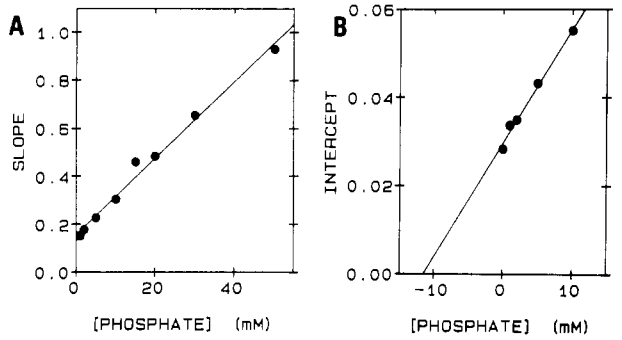

FIGURE 6: Inhibition of the dynein ATPase by phosphate. (A) The slopes of the curves from the reciprocal plot are shown as a function of the phosphate concentration. (B) The intercepts of the curves of the reciprocal plot are shown as a function of the phosphate concentration.

for ATP hydrolysis and ATP synthesis (Holzbaur & Johnson, 1986).

This kinetic analysis of the dynein ATPase pathway can be used to construct a thermodynamic description of the system. All free energies have been calculated under physiological conditions, with 10^{-3} M ATP, 10^{-5} M ADP, and 10^{-3} M phosphate. An equilibrium constant for ATP binding to dynein of 3×10^7 M^{-1} has been determined previously (Holzbaur & Johnson, 1986), which corresponds to a free energy change of −6.2 kcal/mol. Rates of ATP hydrolysis and ATP synthesis at the active site were initially determined from chemical quench flow and oxygen exchange studies (Johnson, 1983; Holzbaur & Johnson, 1986). More recent rapid quench experiments using more purified dynein and an improved quench flow apparatus have lead to refinement of the estimate of the rate of ATP hydrolysis. According to the parameters summarized in Table II, an equilibrium constant for ATP hydrolysis of 3 and a free energy change of −0.7 kcal/mol can be calculated. The equilibrium constants for phosphate release and ADP release are 10^{-2} and 10^{-4} M, respectively, as determined by product inhibition and oxygen exchange studies. The corresponding free energy changes are −1.3 and −2.0 kcal/mol, respectively. The sum of these free energy changes in −10.2 kcal/mol (Table II).

Rosing and Slater (1972) have determined that $\Delta G°$ for the hydrolysis of ATP is −7.53 kcal/mol, such that $\Delta G = -14.4$ kcal/mol under the physiological conditions described above. A comparison of the sum of the free energy changes with this value shows a discrepancy of 4.2 kcal/mol. This could be due to the combined errors of the individual determinations. However, it is also likely that the model upon which the calculations are based is an oversimplification of the true kinetic pathway for the dynein ATPase. There may be one or more kinetic steps which are unaccounted for. Specifically, ADP release may occur in two steps involving a change in conformation of the dynein–ADP state ($D–ADP_1 \rightarrow D–ADP_2$) with a free energy change of −4.2 kcal/mol which precedes the release of ADP. Such a change would not be detected in our attempts to measure the K_d for ADP and would not be measurable in terms of the exchange kinetics. However, this change in conformation could have profound implications for the coupling mechanism. Indeed, if ADP release is rate limiting, a large change in free energy due to ADP release is required for mechanochemical coupling according to the pathway shown in Scheme II.

Valuable insights can be obtained from an analysis of our current understanding of the free energy changes of the system.

Scheme II

$$D + ATP \underset{k_{-1}}{\overset{k_1}{\rightleftharpoons}} D–ATP \underset{k_{-2}}{\overset{k_2}{\rightleftharpoons}} D–ADP–P_i \underset{k_{-3}}{\overset{k_3}{\rightleftharpoons}}$$
$$D–ADP_1 \underset{k_{-4}}{\overset{k_4}{\rightleftharpoons}} D–ADP_2 \underset{k_{-5}}{\overset{k_5}{\rightleftharpoons}} D + ADP$$

The major change in free energy occurs upon the binding of ATP; hydrolysis then occurs near equilibrium, and the remaining free energy is lost upon product release. These observations fit our current model for the crossbridge cycle of the microtubule–dynein ATPase pathway and also confirm the general principles of free energy transduction in biological systems proposed by Jencks (1980) and by Eisenberg and Hill (1985). The large change in free energy upon the binding of ATP is required to dissociate the tightly bound microtubule–dynein complex. The hydrolysis of the bound ATP in a catalytic step near equilibrium conserves the free energy of the system. The free energy changes upon product release can then be coupled to drive the vectoral process of the sliding of adjacent microtubules in the axoneme.

References

Barclay, R., & Yount, R. G. (1972) *J. Biol. Chem. 247*, 4098–4100.

Blum, J. J., & Hayes, A. (1974) *Biochemistry 13*, 4290–4298.

Chilcote, T. J., & Johnson, K. A. (1986) *J. Cell Biol. 103*, 3a.

Clutter, D., & Johnson, K. (1986) *J. Cell Biol. 103*, 1a.

Domanico, P. L., Rahil, J. F., & Benkovic, S. J. (1985) *Biochemistry 24*, 1623–1628.

Eisenberg, E., & Hill, T. L. (1985) *Science (Washington, D.C.) 227*, 999–1006.

Feldhaus, P., Frohlich, T., Goody, R. S., Isakov, M., & Schirmer, R. H. (1975) *Eur. J. Biochem. 57*, 197–204.

Gibbons, B. H., Tang, W. J. Y., & Gibbons, I. R. (1985) *J. Cell Biol. 101*, 1281–1287.

Hackney, D. D. (1980) *J. Biol. Chem. 255*, 5320–5328.

Hackney, D. D., & Clark, P. K. (1985) *J. Biol. Chem. 260*, 5505–5510.

Hackney, D. D., Stempel, K. E., & Boyer, P. D. (1980) *Methods Enzymol. 64*, 60–83.

Holzbaur, E. L. F., & Johnson, K. A. (1986) *Biochemistry 25*, 428–434.

Jencks, W. P. (1980) *Adv. Enzymol. Relat. Areas Mol. Biol. 51*, 75–106.

Johnson, K. A. (1983) *J. Biol. Chem. 258*, 13825–13832.

Johnson, K. A., & Wall, J. S. (1983) *J. Cell Biol. 96*, 669–678.

Kuleva, N. V., Shanina, N. A., & Krasovskaya, I. E. (1983) *Biochemistry (Engl. Transl.) 48*, 1459–1464.

Lanzetta, P. A., Alvarez, L. J., Reinach, P. S., & Candia, O. A. (1979) *Anal. Biochem. 100*, 95–97.

Levy, H. M., & Koshland, D. E. (1959) *J. Am. Chem. Soc. 234*, 1102–1107.

Lienhard, G. E., & Secemski, I. I. (1973) *J. Biol. Chem. 248*, 1121–1123.

Mokrash, L. C., Caravaca, J., & Grisola, S. (1960) *Biochim. Biophys. Acta 37*, 442–447.

Omoto, C. K., & Johnson, K. A. (1986) *Biochemistry 25*, 419–427.

Otokawa, M. (1973) *Biochim. Biophys. Acta 292*, 834–836.

Porter, M. E., & Johnson, K. A. (1983) *J. Biol. Chem. 258*, 6575–6581.

Risley, J. M., & Van Etten, R. L. (1978) *J. Labelled Compd. Radiopharm. 15*, 533–538.

Rosing, J., Slater, E. C. (1972) *Biochim. Biophys. Acta 267*, 275–290.

Sharp, T. R., & Benkovic, S. (1979) *Biochemistry 18*, 2910–2916.
Shimizu, T. (1979a) *J. Biochem. 85*, 1421–1426.
Shimizu, T. (1979b) *J. Biochem. 86*, 1139–1145.
Shimizu, T., & Kimura, I. (1974) *J. Biochem. 76*, 1001–1008.
Shimizu, T., & Kimura, I. (1977) *J. Biochem. 82*, 165–173.
Shimizu, T., & Johnson, K. A. (1983a) *J. Biol. Chem. 258*, 13833–13840.
Shimizu, T., & Johnson, K. A. (1983b) *J. Biol. Chem. 258*, 13841–13848.
Shimizu, T., & Katsura, T. (1988) *J. Biochem. 103*, 99–105.
Shimizu, T., & Johnson, K. A. (1989) *Biochemistry* (in press).
Shimizu, T., Kaji, K., & Kimura, I. (1977) *J. Biochem. 82*, 1145–1153.
Sleep, J. A., Hackney, D. D., & Boyer, P. D. (1978) *J. Biol. Chem. 253*, 5235–5238.
Sleep, J. A., Hackney, D. D., & Boyer, P. D. (1980) *J. Biol. Chem. 255*, 4094–4099.
Weeds, A. G., & Taylor, R. S. (1975) *Nature (London) 257*, 54–56.
Weeds, A. G., & Pope, B. (1976) *J. Mol. Biol. 111*, 129–157.

Novel Methyl Transfer during Chemotaxis in *Bacillus subtilis*†

Mark S. Thoelke, John R. Kirby, and George W. Ordal*
Department of Biochemistry, School of Chemical Sciences and College of Medicine, University of Illinois, Urbana, Illinois 61801
Received December 2, 1988

ABSTRACT: If *Bacillus subtilis* is incubated in radioactive methionine in the absence of protein synthesis, the methyl-accepting chemotaxis proteins (MCPs) become radioactively methylated. If the bacteria are further incubated in excess nonradioactive methionine ("cold-chased") and then given the attractant aspartate, the MCPs lose about half of their radioactivity due to turnover, in which lower specific activity methyl groups from *S*-adenosylmethionine (AdoMet) replace higher specific activity ones. Due to the cold-chase, the specific activity of the AdoMet pool is reduced at least 2-fold. If, later, the attractant is removed, higher specific activity methyl groups return to the MCPs. Thus, there must exist an unidentified methyl carrier that can "reversibly" receive methyl groups from the MCPs. In a similar experiment, labeled cells were transferred to a flow cell and exposed to addition and removal of attractant and of repellent. All four kinds of stimuli were found to cause methanol production. Bacteria with maximally labeled MCPs were exposed to many cycles of addition and removal of attractant; the maximum amount of radioactive methanol was evolved on the third, not the first, cycle. This result suggests that there is a precursor–product relationship between methyl groups on the MCPs and on the unidentified carrier, which might be the direct source of methanol. However, since no methanol was produced when a methyltransferase mutant, whose MCPs were unmethylated, was exposed to addition and removal of attractant or repellent, the methanol must ultimately derive from methylated MCPs.

In a number of species of bacteria, certain membrane proteins, termed methyl-accepting chemotaxis proteins (MCPs), act as transducers which undergo reversible methyl esterification of glutamate residues in response to binding of chemical attractants or repellents (Goldman et al., 1982; Kort et al., 1975; Springer et al., 1977; Kleene et al., 1977; Van Der Werf & Koshland, 1977). In *Escherichia coli*, this modification is thought to play a role in adaptation (Springer et al., 1977; Goy et al., 1977). During adaptation, the bacteria swim smoothly, methylation of MCPs occurs, and methanol production ceases. Eventually, the bacteria return to random behavior, net methylation of MCPs no longer changes, and the basal level of methanol production resumes. On removal of attractant, the bacteria transiently tumble, MCPs are demethylated, and methanol production is briefly enhanced. Repellents have the opposite effects as attractant on methylation of MCPs and on methanol production (Springer et al., 1977; Toews et al., 1979; Kehry et al., 1984). The methyl donor for the MCPs is *S*-adenosylmethionine (AdoMet) (Springer & Koshland, 1977).

In vitro experiments in *Bacillus subtilis* have shown that the methyl donor for MCPs is AdoMet (Burgess-Cassler et al., 1982) and that glutamate side chains are methylated (Ahlgren & Ordal, 1983). However, the metabolic events that occur following addition of attractant are quite different in the two species of bacteria. Addition of the attractant aspartate to *B. subtilis* causes an immediate redistribution of methyl groups, a flux of methyl groups through the MCPs, and a period of increased methanol production (Goldman et al., 1982; Thoelke et al., 1988). The fact that radioactive methyl groups are immediately lost from MCPs but only gradually emerge as methanol implies that methyl groups are first transferred to an intermediate carrier before evolving as methanol (Thoelke et al., 1988).

Thus, the effect of addition of attractant to *B. subtilis* is different from its effect on *E. coli*. We next wished to investigate the effects of removal of attractant on MCP methylation and methanol formation.

Experimental Procedures

Strains. B. subtilis strain OI1085 (*trpF7 hisH2 metC*) is wild type for chemotaxis (Ullah & Ordal, 1981). Strain OI1100 is its *cheR* derivative and lacks methyltransferase (Ullah & Ordal, 1981).

E. coli strain RP437 (F^- *thi thr leu his met eda-50 thr-1 rpsL*) is wild type for chemotaxis (Slocum & Parkinson, 1985).

†Supported by National Institutes of Health Grant AI20336 and National Science Foundation Grant DCB 85-01604.

0006-2960/89/0428-5585$01.50/0 © 1989 American Chemical Society